Available online at www.sciencedirect.com

ScienceDirect

MATTER AND RADIATION AT EXTREMES

Matter and Radiation at Extremes 2 (2017) 37–54

www.journals.elsevier.com/matter-and-radiation-at-extremes

Review article

# Laser-direct-drive program: Promise, challenge, and path forward

E.M. Campbell [a,*], V.N. Goncharov [a], T.C. Sangster [a], S.P. Regan [a], P.B. Radha [a], R. Betti [a], J.F. Myatt [a], D.H. Froula [a], M.J. Rosenberg [a], I.V. Igumenshchev [a], W. Seka [a], A.A. Solodov [a], A.V. Maximov [a], J.A. Marozas [a], T.J.B. Collins [a], D. Turnbull [a], F.J. Marshall [a], A. Shvydky [a], J.P. Knauer [a], R.L. McCrory [a], A.B. Sefkow [a], M. Hohenberger [b], P.A. Michel [b], T. Chapman [b], L. Masse [b], C. Goyon [b], S. Ross [b], J.W. Bates [c], M. Karasik [c], J. Oh [c], J. Weaver [c], A.J. Schmitt [c], K. Obenschain [c], S.P. Obenschain [c], S. Reyes [b], B. Van Wonterghem [b]

[a] *Laboratory for Laser Energetics, University of Rochester, Rochester, NY, USA*
[b] *Lawrence Livermore National Laboratory, Livermore, CA, USA*
[c] *Naval Research Laboratory, Washington, DC, USA*

Received 25 January 2017; accepted 7 March 2017
Available online 19 March 2017

**Abstract**

Along with laser-indirect (X-ray)-drive and magnetic-drive target concepts, laser direct drive is a viable approach to achieving ignition and gain with inertial confinement fusion. In the United States, a national program has been established to demonstrate and understand the physics of laser direct drive. The program utilizes the Omega Laser Facility to conduct implosion and coupling physics at the nominally 30-kJ scale and laser–plasma interaction and coupling physics at the MJ scale at the National Ignition Facility. This article will discuss the motivation and challenges for laser direct drive and the broad-based program presently underway in the United States.


*PACS Codes:* 52.5; 52.57.Fg; 52.38; 52.38.Bv; 52.38.Mf

*Keywords:* Inertial fusion; Direct drive; Laser interactions; Hydrodynamics; Omega; National ignition facility

## 1. Introduction

In inertial confinement fusion (ICF), encapsulated fusion fuel is compressed and heated to extreme density, temperature, and pressure so that the fusion reaction rate is rapid enough that significant energy release can take place before the fuel disassembles [1]. Depending on the details of the implosion such as fuel mass and implosion geometry and whether magnetic fields are employed, required fuel pressures can range from tens to hundreds of gigabars. In the majority of present fusion research, the fuel is an equal molar mixture of deuterium and tritium (DT) and an ion temperature of ~5 keV is required to initiate the fusion reactions with corresponding particle densities for the various ICF target concepts ranging from ~$2 \times 10^{24}$ to $2 \times 10^{26}$ ions/cm$^3$. Drivers such as lasers and pulsed-power systems that compress energy in space and time are required to produce such extreme conditions in the laboratory [2]. The concentrated energy flux from these systems generates pressure on the exterior of the target that implodes the fuel to the conditions required for fusion. In laser direct drive (LDD) [3], the pressure is produced by the rapid ablation of the outer target surface of a spherical target by the high-intensity laser pulse. In laser indirect drive (LID) [4], the

* Corresponding author.
*E-mail address:* mcamp@lle.rochester.edu (E.M. Campbell).
Peer review under responsibility of Science and Technology Information Center, China Academy of Engineering Physics.

http://dx.doi.org/10.1016/j.mre.2017.03.001

laser energy is first converted into sub-kilovolt X-rays that then ablate the outer surface of the capsule. To maximize the implosion efficiency, the ablators are low-$Z$ materials such as plastic and carbon. In LDD, to maximize the efficiency of the implosion, most of the ablated mass is DT. With pulsed power, the magnetic pressure generated by multi-mega-amp currents flowing through a cylindrical target drives the implosion [5]. For all of these schemes, the pressures are in the range of one to several hundred megabars and the implosion effectively serves as a "pressure amplifier" to produce the fuel conditions required for fusion. In both laser approaches these pressures produce implosion velocities $v_{\mathrm{imp}}$ in excess of $3.5 \times 10^7$ cm/s ($>10^{-3}$ of light speed). Depending on the pulsed-power target concept, $v_{\mathrm{imp}}$ can be somewhat slower with values $>10^7$ cm/s. The three target concepts are shown in Fig. 1.

In D–T fusion, a total of 17.6 MeV of energy is released per reaction and carried off by a 14.1-MeV neutron and a 3.5-MeV alpha particle [1–4]. The energetic uncharged neutron readily escapes the plasma [6] (the range (areal density) in terms of parameters used in ICF as described below is ~10 g/cm$^2$). In contrast, if the plasma is sufficiently dense, the alpha particles can be stopped in the plasma, where they deposit their energy and rapidly heat the fuel. When this occurs, the fusion reaction rate rapidly increases (the reaction rate scales ~ $T^2$ to $T^4$ for ion temperatures of interest [7] and the energetics of the plasma becomes dominated by alpha self-heating). For this to occur in unmagnetized plasmas, the product of the areal density and ion temperature of the fuel, $\rho RT_{\mathrm{i}}$, must exceed 0.3 g/cm$^2$ × 5 keV [1–4]. This generalized Lawson criteria in ICF is equivalent to the $n\tau T_{\mathrm{i}}$ of magnetic fusion, where $\tau$ is the energy confinement time and $n$ is the particle density. This can be readily seen for ICF since the inertial confinement time will be proportional to the imploded fuel radius. Recent so-called "high-foot" LID implosions [8] at the National Ignition Facility (NIF) have achieved implosions where alpha heating has begun to dominate the hot-spot energetics. In these NIF experiments, alpha heating produced a doubling of the fusion yield that would have resulted if only energy from the implosion was considered. While not yet achieving ignition, this is an important step in ICF and for all fusion research.

Advances in pulsed power over the past several decades have led to promising concepts in ICF such as MagLIF (magnetized liner inertial fusion) [5] that employs embedded magnetic fields in laser preheated plasmas, which then undergo a cylindrical implosion driven by the force produced by the interaction of the multi-mega-amp current from the pulsed-power driver and the self-generated magnetic field [Fig. 1(c)]. The cylindrical targets of MagLIF are a well-matched load and target concept to the pulsed-power driver. The magnetic Reynolds number ($R_{\mathrm{m}}$) of these plasmas is high enough to freeze the $B$ field in the plasma and can rapidly increase as the plasma implodes and is compressed. Even with loss mechanisms such as the Nernst effect [9], the field can be enhanced by several orders of magnitude, not only reducing electron thermal losses but also trapping the fusion alpha particles. Initial fields of 10 T ($10^5$ G) can be amplified by implosion to ~100 MG. With fields this large, even the alpha particles with low fuel $\rho R$ can be trapped by the magnetic field. This will occur when the Lamor radius of the alpha particles is less than the imploded fuel radius. For example, at 100 MG, the Lamor radius of the 3.5-MeV alpha particles is 27 μm. In this case, the product of the magnetic field and fuel radius, $BR$, is the important parameter. Detailed simulations show that values of ~0.6 MG-cm will be sufficient to see significant alpha heating of the plasma with the majority of the $p\delta V$ work of the implosion compressing the fuel (and not the $B$ field) [5].

It should be noted that there are also potential advantages to employing $B$ fields in laser-driven ICF [10,11]. Applied $B$ fields in hohlraums used in LID can reduce electron conductivity, increasing the electron temperature $T_{\mathrm{e}}$, and subsequently increasing Landau damping, thereby reducing deleterious laser–plasma interaction processes and increasing the propagation distance in the hohlraum. In addition, if embedded $B$ fields can be enhanced in the capsule implosion, electron transport losses and even alpha trapping can occur and improve the overall fusion performance. Early research has been encouraging but much work remains to be done [10,11]. For example, laser-direct-drive implosions on OMEGA have shown ~30% yield enhancements when an external $B$ field was applied and amplified in the implosion [11].

For many applications, high gain (defined as the ratio of the fusion energy output to the incident driver energy) must be large. For example, in fusion energy applications, to have an economically viable plant, the product of driver efficiency and

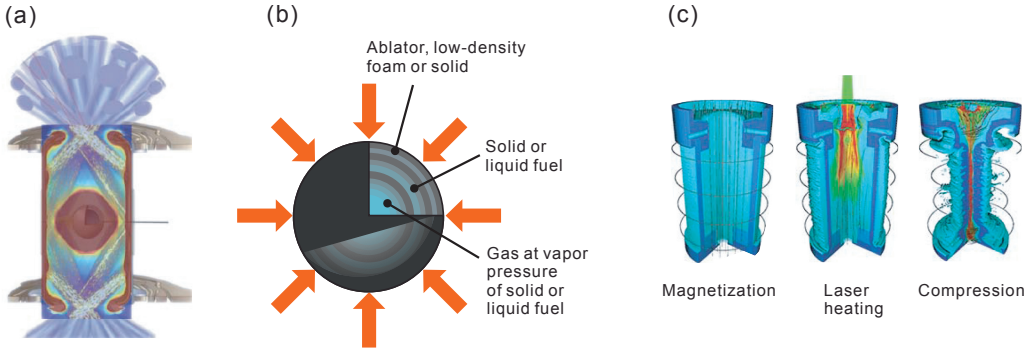


Fig. 1. Inertial confinement fusion (ICF) concepts: (a) laser indirect drive (LID); (b) laser direct drive (LDD); and (c) magnetized liner inertial fusion (MagLIF).

target gain must be greater than ~10 [12]. Fusion energy studies show that this will result in an acceptably low (<25%) plant recirculating power (the required power needed for the driver and the additional plant needs). With significant research, future laser drivers may have efficiencies in the range of 10%−20% requiring fusion gains ~50.

To achieve such gains, as described below, to minimize the driver energy, the igniting plasma must be surrounded by cold, nearly Fermi-degenerate fuel, where the DT pressure and density are related by $P_{\mathrm{Fermi}} \sim \rho^{5/3}$. For the fuel to be degenerate, the quantity $T(\mathrm{eV})^2/\rho(\mathrm{g})^{4/3}$ must be ~1; if not, finite temperature corrections on the specific energy are required [4]. The surrounding cold fuel confines (tamps) the igniting central hot spot and provides the fusion fuel that results in high yield and gain. At ignition, a thermonuclear burn wave initiated from the hot spot propagates into the cold fuel, producing high gain and fusion yield. The minimum specific energy required to compress the cold fuel encompassing the hot spot occurs when the minimum entropy is added during an implosion. When the fuel is Fermi degenerate [1], the specific energy required for compression is approximately given by $\varepsilon_{\mathrm{Fermi}}$ ($j/g$) ~ $3 \times 10^5\ \rho^{2/3}$ (g/cm$^3$). The fuel adiabat ($\alpha$) that describes the ratio of the fuel pressure to the Fermi-degenerate value [1,2,4] is a measure of the deviation from the minimum compression energy. The main fuel pressure in an imploding target can be raised above the Fermi limit by shocks, energetic electrons, or high-energy photons. High-gain ICF target designs typically have a main fuel adiabat of less than 2 to 3 [2−4].

As described in Sec. 2 below, the overall efficiency in which the energy from the ICF drivers is coupled to the fusion fuel is very low. In order to maximize the mass of DT that can be imploded, the implosion dynamics are chosen to both ignite the fuel and compress a sufficient mass that will release a significant amount of energy. It can be readily shown that the fraction of the fuel in unmagnetized ICF targets that undergoes fusion (the burnup fraction $\phi$) depends on the total fuel areal density and ion temperature [1,2,4]:

$$\phi = \rho R/[\rho R + f(T_{\mathrm{i}})], \tag{1}$$

where $f$ ($T_{\mathrm{i}}$) is ~6 for ion temperatures of interest. Given optimistic but credible driver energies, fuel masses, and implosion physics, $\rho R$ values of 3 should be ultimately possible, resulting in a burnup fraction of 1/3. This would be a long-term credible goal for the ICF Program. Given that the fusion energy release from a gram of equimolar DT is ~$4 \times 10^{11}$ J/g [2,4], to release 100 MJ of energy if 1/3 of the DT underwent fusion would require ~750 μg of fuel to be heated and compressed. To heat that amount of fuel to 5 keV would require ~375 kJ coupled to the fuel (the specific heat of DT is ~100 MJ/keV-g) [1−4]. To put this in perspective, the 1.8-MJ NIF laser at Lawrence Livermore National Laboratory (LLNL) [13] at present with laser-indirect-drive targets couples ~10−20 kJ to the compressed fuel (hot spot and main fuel) [8]. In contrast, the minimum energy to compress 750 μg of DT to 1000 g/cm$^3$ (the nominal peak density of the cold shell is ~1000 g/cm$^3$) is ~22.5 kJ or ~6% of that required to heat an equivalent mass to 5 keV.

This simple energetics argument defines the implosion strategy commonly used in high-gain, laser-driven ICF target designs. The implosion is designed so that a small fraction (~5%) of the fuel mass is compressed and heated to satisfy the generalized Lawson criteria to ignite and to propagate a fusion "burn wave" into the majority of the fuel, which must be maintained as close as possible to Fermi degeneracy. The target and driver temporal pulse format are designed so that the partition of the implosion energy between the igniting hot spot and cold fuel is approximately equal [2,4].

In the United States, as shown in Fig. 2, three major facilities presently conduct research in ICF: the NIF at LLNL [13], the Omega Laser Facility at the Laboratory for Laser Energetics (LLE) [14] of the University of Rochester, and the Z facility at Sandia National Laboratories (SNL) [15]. The NIF can deliver up to 1.8 MJ and 500 TW of 0.35-μm laser light to a target in 192 beams and is presently configured to illuminate indirect-drive (X-ray) targets. The 60-beam OMEGA laser can deliver up to ~30 kJ and 30 TW of 0.35-μm laser light in a symmetric configuration optimized for direct-drive targets, and the ~26-MA pulsed-power Z facility can deliver ~1 MJ and 80 TW to a load and is the primary facility to study pulsed-power target concepts such as MagLIF. Smaller facilities such as the NIKE [16] KrF laser at the Naval Research Laboratory (NRL) also contribute to fundamental ICF research but are not configured or energetic enough to conduct implosion experiments.

At the initiation of the NIF project by the U.S. Department of Energy in 1994, the only ICF target concept that had a sufficient database, primarily from the ten-beam, 30- to 40-kJ, 0.35-μm NOVA [17] laser at LLNL to establish the facility baseline requirements, was laser indirect drive. At the time in the early 1990s, the OMEGA laser was being upgraded to 60 beams and just beginning operations (OMEGA with 60 beams was completed in 1996) and pulsed-power research was focused on light ion beams. Today progress in laser direct drive and pulsed power as well as the progress and challenges identified on NIF with laser indirect drive has resulted in three viable approaches to ICF [18]. Each has advantages and challenges but the diversity of approaches should be considered a positive development in the field since the beginning of the NIF.

This article presents the national direct-drive program currently underway in the United States. The program involves research done primarily on the OMEGA and NIF lasers operating at 0.35 μm. As mentioned above, the 0.248-μm KrF NIKE laser at NRL also conducts important laser-direct-drive research in planar geometry. Planar-target experiments are also conducted on the OMEGA EP laser at LLE with four NIF-like beams. The paper is organized as follows: Sec. 2 motivates the laser-direct-drive program along with its advantages and challenges; Sec. 3 describes the status and plans for LDD research on the OMEGA laser and on the NIF in its present LID configuration; and Sec. 4 presents conclusions and an overall outlook for laser direct drive. It should be noted that this article

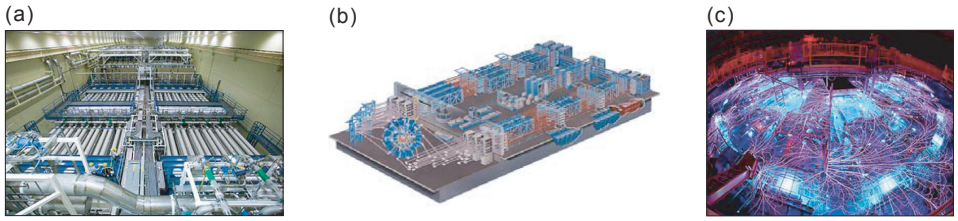


Fig. 2. (a) The National Ignition Facility; (b) the OMEGA Laser System; and (c) the Z Pulsed-Power Facility.

focuses on the present mainline approach to laser direct drive (i.e., hot-spot ignition with unmagnetized fuel). In addition to this most-studied ICF design, other concepts have been identified that "separate" compression and heating. The fast-ignition concept [19] first compresses the fuel and then uses an additional source of energetic particles (electrons or ions) to heat and ignite the fuel. In shock ignition [20], the compressed fuel is ignited by a strong shock launched near the end of the implosion. A hybrid concept is under study where a thin, high-$Z$ overcoat enables early-time X-ray drive followed by conventional direct drive after the laser burns through the high-$Z$ layer. In addition to these "single-shell" designs, there is growing interest in multiple-shell capsules [21,22]. In this approach, an outer shell is irradiated by the driver that then impacts an interior shell (or shells), imparting some of its kinetic energy that subsequently implodes the fusion fuel. Despite the complexity of target fabrication, interest is growing in these multiple-shell concepts since they potentially have attractive hydrodynamic and burn physics features. The status and plans of these approaches will be discussed in future articles.

It is also important to recognize that research and the facilities, diagnostics, and modeling motivated by ICF have also enabled the development of the physics of matter at extreme conditions—high-energy-density physics (HEDP) [23] in the laboratory. This area is an emerging field with a broad and growing scientific interest with impact in condensed matter, planetary and stellar science, radiation physics, nuclear physics, and astrophysics.

## 2. Motivation for direct drive

### 2.1. Laser-direct-drive advantages

The main motivation for laser direct drive is the increased coupling of the driver energy to the target, enabling more mass to be imploded to the conditions necessary for fusion [2,3,24]. The importance of this can be readily seen from the generalized Lawson criteria for the hot spot. Relating the threshold hot-spot areal density and temperature $\rho RT_{\rm th}$ to the pressure and energy, it is straightforward to show that the hot-spot pressure $P_{\rm hs}$ must exceed [24] a threshold value $P_{\rm th}$ for ignition:

$$P_{\rm hs} > P_{\rm th} = 250\ {\rm Gbar}(E_{\rm hs}/10\,{\rm kJ})^{-1/2}, \qquad (2)$$

where $E_{\rm hs}$ is the driver energy that is coupled to the hot spot. By coupling more energy into the hot spot, the required pressure and thus fuel convergence for ignition is reduced (the hot-spot radius $R_{\rm hs}$ scales as $(E_{\rm hs})^{1/2}$). This simple relation, illustrated in Fig. 3, shows the advantage of imploding more fuel mass made possible by coupling more driver energy. Ignition/gain LDD targets at the NIF scale can potentially couple 30–40 kJ into the hot spot, and at this coupled energy, ignition requires hot-spot pressures <150 Gbar and a convergence (defined as the ratio of the initial outer fuel radius to the hot-spot radius) of <25 [3,4,24]. As discussed below, the total energy coupled to the fuel (hot spot and main fuel) for direct drive can reach up to 100 kJ at NIF-scale driver energies.

In laser direct drive the overall efficiency in which the laser energy is delivered to the fuel is a product of three terms: the absorption efficiency, the rocket efficiency, and the efficiency in which the kinetic energy of the imploding target is converted into internal energy of the fuel at stagnation [2–4]. As mentioned above for high-gain targets, the energies in the hot spot and cold fuel are approximately equal. A nominal LDD target and laser pulse shape designed to achieve ignition and modest gain at an incident energy of 1.5 MJ at a laser wavelength of 0.35 μm is shown in Fig. 4 [24]. For this design, the peak incident laser intensity summed over multiple beams is ~$10^{15}$ W/cm$^2$. The spherical divergence of the plasma flow will result in a plasma corona (for $n_{\rm e} < n_{\rm c}$ where $n_{\rm c} \sim 1.1 \times 10^{21}/(\lambda_{\mu{\rm m}})^2$) with the scale length a fraction (~1/3) of the capsule radius (~600 μm). At these intensities, laser wavelength, and plasma scale length, the target absorption will occur primarily by inverse bremsstrahlung (collisional) absorption [25]. In the absence of any laser–plasma instabilities, absorption efficiencies greater than 80% would be expected.

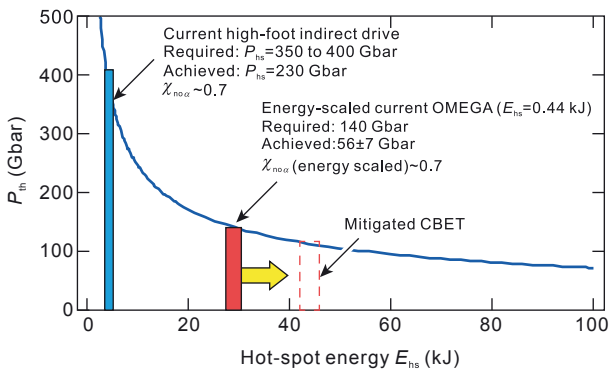


Fig. 3. Threshold hot-spot pressure versus energy in hot spot with and without CBET scaled to NIF energies (1.5–1.8 MJ). Inferred pressure from the "high-foot" campaign on the NIF is also indicated as well as the ignition parameter $\chi_{{\rm no}\ \alpha}$.

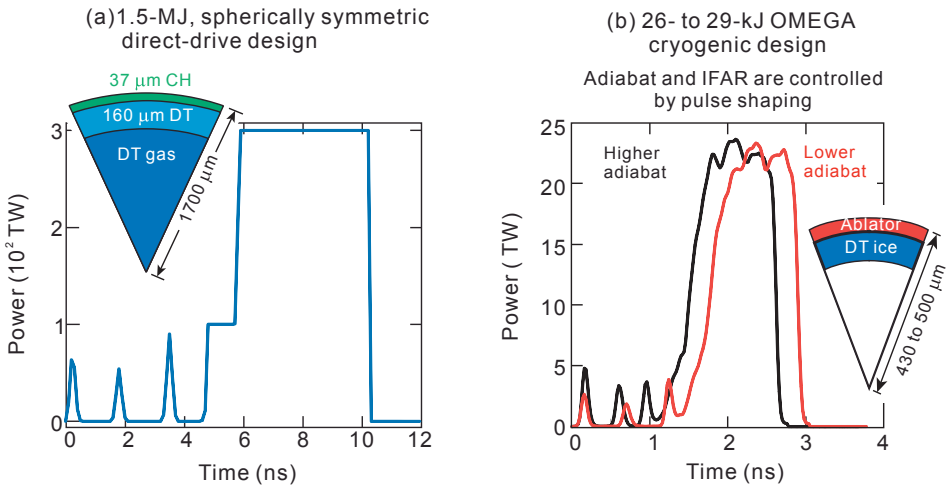


Fig. 4. (a) NIF-scale direct-drive–ignition target and (b) hydrodynamically scaled targets for OMEGA.

However, as we discuss below, the multibeam irradiation of LDD enables processes (such as cross-beam energy transport (CBET)) to take place that can significantly reduce the target absorption [26]. CBET is simply stimulated Brillouin scattering (SBS) in which an incoming laser beam that is refracted in the underdense corona or reflected/scattered off the critical surface serves as an SBS "seed" for incoming light from another laser beam.

The absorbed laser energy rapidly ablates the outer surface of the capsule, and the outwardly expanding momentum of the plasma drives the remaining mass inward as a spherical rocket with an implosion velocity $v_{\mathrm{imp}}$. The implosion velocity is related to the ablated plasma exhaust velocity $U_{\mathrm{exh}}$ by the rocket equation $v_{\mathrm{imp}} = U_{\mathrm{exh}} \ln(M_0/M_{\mathrm{f}})$, where $(M_0/M_{\mathrm{f}})$ is the ratio of the initial to final target mass. The rocket efficiency, defined as the ratio of the imploding capsule's kinetic energy to the absorbed laser energy, is reduced from that expected from the simple rocket equation (which maximizes at ~60% when $M_{\mathrm{f}}/M_0$ is ~0.2) because the laser (or X-rays) continuously heats the plasma exhaust [2–4]. In laser direct drive, the rocket efficiency is also reduced since the absorbed energy must be conducted from the absorption region ($n_{\mathrm{e}} < n_{\mathrm{c}}$) to the ablation surface [2–4]. Simple estimates and numerical simulations give values in the range of 5%–10% depending on the laser intensity, ablator material, wavelength, and electron-transport models. Typical values for laser-direct-drive–ignition designs are in the range of 7%–10% [2,3]. The rocket efficiency is somewhat higher for laser indirect drive (~15%) [4] as a result of the drive energy being deposited at higher densities near the ablation surface and ablating more mass at a lower exhaust velocity (the exhaust velocity is better matched to the implosion velocity).

At the final stages of the implosion, when the pressure in the hot spot exceeds that of the incoming shell, a strong shock is launched into the shell, decelerating it. The kinetic energy of the shocked region of the shell constitutes the final $p\delta V$ work to the hot spot [24]. The unshocked free-falling region of the DT does not contribute to the hot spot's internal energy. Including all of these factors, analytic models and detailed simulations show that it is possible, as mentioned above, with NIF-scale energies (~1.5 MJ) to couple ~30–40 kJ into the hot spot; as shown in Fig. 3, this translates into threshold pressures in the range of 120–140 Gbar and a hot-spot convergence of ~20. The total energy coupled to the fuel (hot spot and main fuel) is predicted to reach as high as ~100 kJ for NIF-scale energies if CBET is mitigated. The large fuel mass (~1 mg) imploded in direct-drive targets, once ignited, can produce multi-megajoule fusion output and high fusion gain (>25). However, as discussed below (Sec. 2.2), deviations from a 1-D implosion such as spatial variations in ablation pressure can also result in an incomplete conversion of kinetic energy into internal energy at stagnation, further reducing the overall implosion efficiency of the system and preventing fusion conditions in the hot spot from being reached [24].

For a given laser driver energy, laser direct drive couples ~5 times more energy to the fuel than indirect drive [2–4]. In indirect drive the laser irradiates the high-$Z$ (typically Au or U) hohlraum, converting a significant fraction of the laser energy into X-rays as shown in Fig. 2. Depending on the details of the hohlraum design, the hohlraum absorption efficiency can range from ~80% to >95% with ~80% of the absorbed energy converted into X-rays approximated as a blackbody with an effective radiation temperature from ~250 eV to 300 eV [4,8]. A fraction of the laser energy (~10%–15%) also resides in penetrating M-shell radiation (transitions to the $n = 3$ shell at ~2.5 keV for Au). These higher-energy photons can preheat the fuel, so designs using appropriate mid-$Z$ dopants must be placed in the ablators. The largest impact on reducing the driver's overall energy efficiency to the capsule is the geometric loss—the hohlraum/capsule area ratio (the "case-to-capsule" ratio) [4]. This must be sufficiently large so that low-order-mode drive asymmetries (the radiation nonuniformity is decomposed into spherical harmonics with $\ell$ modes where $\ell = kR$ with $R$ being the capsule radius and $k$ the wave number of the mode [4]) are small enough so that the large capsule convergences (30–40)

needed to achieve the pressures required for fusion are obtained. This case-to-capsule ratio can be as large as ~15 to 30. X-ray energy also escapes through the laser entrance holes, and the capsule also re-radiates some of the incident X-ray flux.

While the rocket efficiency of X-ray drive is larger than electron-driven ablation, all of the above processes result in ~10–20 kJ into the stagnated fuel for present designs with 1.8 MJ of incident laser energy to the hohlraum [8]. As shown in Fig. 3, hot-spot pressures for ignition for these more limited mass targets (the approximate total fuel mass is ~200 μg) are then ~350 Gbar, requiring convergences in excess of 35 [8,27]. It is important to note that X-ray–driven targets at the NIF, while not yet achieving ignition, have been imploded to inferred hot-spot pressures of ~230 Gbar [8]. If such pressures were obtained with more massive laser-direct-drive targets, robust ignition would be expected. Research in laser indirect drive to improve the coupled energy to the fuel is ongoing but direct drive will maintain this benefit (increased energy coupling) for all laser approaches.

In addition to the larger fuel mass and its implosion implications, LDD has several other potentially attractive features. To achieve the required initial ablation pressures ($P_{\mathrm{abl}}$ ~ 100 Mbar), peak laser on-target intensities are in the range of $10^{15}$ W/cm$^2$ (simple steady-state analytic models give $P_{\mathrm{abl}}(\mathrm{Mbar}) \sim 40(I_{15}/\lambda_{\mu\mathrm{m}})^{2/3}$, where $I_{15}$ is the laser intensity measured in $10^{15}$ W/cm$^2$ and the laser wavelength $\lambda$ is in microns) [2–4]. As previously discussed, laser direct drive utilizes multiple laser beams to get the drive uniformity with this peak intensity so that the individual laser beams are significantly less intense. For example, on OMEGA implosion experiments, the single-beam intensity is only ~3 to $5 \times 10^{13}$ W/cm$^2$ and would be even smaller if more beams were employed. The laser–plasma instabilities (LPI's) that can reduce the target absorption, redirect the laser light, or produce energetic electrons that can preheat the fuel depend on the laser intensity (threshold, growth rate) and, in the case of multibeam overlapping, the interplay and "cooperation" between multiple beams [28–31]. The interplay of multiple beams, however, is a complexity for all laser approaches. As will be described in Sec. 2.2, the most important of the instabilities—stimulated Brillouin scattering (SBS), stimulated Raman scattering (SRS), and the two-plasmon–decay instability ($2\omega_{\mathrm{pe}}$)—can be simply described as a three-wave resonant decay process where the incident laser at frequency $\omega_{\mathrm{L}}$ decays into two daughter waves [25]. The daughter waves can be an electromagnetic wave ($\omega_{\mathrm{scat}}$), a low-frequency ion-acoustic wave ($\omega_{\mathrm{iaw}}$), or a high-frequency electron plasma wave ($\omega_{\mathrm{pe}}$). When one of the daughter waves is a high-frequency electron plasma wave, high-energy electrons with an approximate temperature $T_{\mathrm{hot}}$ ~1/2 $m_{\mathrm{e}}$ $(V_\varphi)^2$, where $V_\varphi$ is the phase velocity of the electron plasma wave $(\omega_{\mathrm{pe}}/k_{\mathrm{epw}})$, can be produced that can preheat the fuel. When one of the daughter waves is an electromagnetic wave, laser energy can be scattered, redirecting the laser energy or reducing the target absorption. The daughter waves for the two-plasmon–decay instability are both electron plasma waves, whereas in SRS, one daughter wave is a scattered electromagnetic (EM) wave and the other is an electron plasma wave [25].

In the case of direct drive, the individual beam intensities are generally below the instability thresholds with the coronal plasma conditions typical of LDD. The instabilities are then driven by a combination of multiple beams. For example, only those beams that share a common daughter wave act together to drive the $2\omega_{\mathrm{pe}}$ instability [28,29]. This enables strategies (polarization, timing, frequency) to minimize LPI and, even when it occurs, to keep it in the "linear regime" where more accurate and less complex models and simulations are to be expected [28].

In contrast, the individual intensities for laser indirect drive are in the range of $5 \times 10^{14}$ W/cm$^2$ to $10^{15}$ W/cm$^2$ [4,31,32]. Overlapped beam intensity can be ~$10^{16}$ W/cm$^2$. These intensities are required so that the laser light can be injected through the entrance holes of the hohlraum, which must be kept as small as possible to eliminate radiation loss through the aperture and to minimize its impact on drive symmetry [4]. In contrast to laser direct drive, the single-beam intensities can exceed the instability thresholds. With these parameters, nonlinear effects (particle trapping, harmonic generation, mode coupling) on the laser–plasma interaction physics will likely occur [2,25,31].

The intensity thresholds for LPI depend on the size and homogeneity of the underdense corona [25], and the relatively small corona limited by the target size is a potential advantage for LDD. For example, the single-beam intensity threshold for the SRS backscattering instability in a plasma with a linear density gradient scale length $L_{\mathrm{n}}$ (μm) and laser wavelength $\lambda$ (μm) that can occur at electron densities $< n_{\mathrm{e}}/4$ is [25,31]

$$I\left[\mathrm{W/cm^2}\right] > 4 \times 10^{17}/(L_{\mathrm{n}}\lambda). \tag{3}$$

With plasma corona scale lengths for ignition targets in for laser direct drive ~600 μm, the laser intensity at 0.35 μm must exceed ~$2 \times 10^{15}$ W/cm$^2$. This intensity is larger than the summed intensity of nominal designs. This simple estimate would imply that SRS backscatter should not be a major issue in LDD. If SRS occurs in LDD, it would be at low levels and likely a result of "hot spots" in the laser irradiation profile, sidescatter, multibeam effects, and a more complicated plasma density profile or laser propagation path in the corona [30]. However, the large plasmas and the challenge of scaling the interaction physics dictate the need for experiments to explore SRS in ignition-scale direct drive coronas.

In contrast to laser direct drive, where the corona is limited by the size of the capsule, in LID the hohlraum underdense plasma is larger (>1000 μm) and with interpenetrating plasma flows (i.e., wall blowoff interacting with the ablated capsule plasma), far more complex [4,31,32]. Not surprisingly, over the history of the ICF Program, SRS has been a major coupling mechanism and a major source of hot electrons in laser indirect drive [4,31]. For example, for the baseline laser drive hohlraum targets of the National Ignition Campaign (NIC) executed at the NIF, SRS levels of ~20% of the incident laser energy were observed to exit the target in the baseline

gas-filled (He gas at a density of ~0.6 mg/cm$^3$) hohlraums [8,32]. The detected level of SRS is most likely an underestimate since the scattered light will be absorbed as it propagates out of the plasma. Recent research with vacuum and near-vacuum (He density ~0.03 mg/cm$^3$) hohlraums has seen a significant reduction in detected SRS and high-energy electron levels [33]. Symmetry control in these low-density hohlraums, however, must be addressed. Varying hohlraum geometry and irradiation strategies that improve symmetry and minimize LPI will be an ongoing research focus for laser indirect drive.

Accurately scaling the laser−plasma interaction, however, has been generally impossible over the history of the ICF Program because of the complexity of the physics. For example, in the 1990's as mentioned previously, the ten-beam, 30- to 40-kJ NOVA laser [17] was the largest facility at the time to explore the physics that would occur at the MJ scale of the NIF. Experience has shown that experimental data at relevant plasma and irradiation conditions are essential. Although not configured and with beam conditioning not optimal for direct drive, the MJ-scale NIF presents a unique opportunity to explore LPI at direct-drive ignition-scale plasma conditions. The LPI challenges and the research program will be discussed in Secs. 2.2 and 3.

Finally, another attractive and important feature of LDD is diagnostic accessibility. This makes it possible to develop and field the field diagnostics that can characterize the plasma corona and laser-driven plasma waves and observe the scattered light, implosion, and stagnation physics in multiple directions. The spherical geometry also enables a limited number of measurements such as scattered-light calorimetry to determine important features such as target absorption. To understand, model, and mitigate LPI, an understanding of the plasma corona conditions ($n_e$, $T_e$, $T_i$, flow velocity, and ion charge state ($Z$)) in time and space is required as well as an understanding of the evolution of the electron and ion waves produced in the laser−plasma interaction. Laser direct drive enables one to employ a number of diagnostics including optical probing (deep UV Thomson scattering and interferometry) as well as optical and X-ray spectroscopy and imaging to characterize the corona and the LPI processes that are present [24,28]. In addition to characterizing the corona, diagnostics that measure the overdense plasma and the implosion physics are facilitated with the open geometry of direct drive. Conventional X-ray backlighting from an external X-ray source is routinely utilized in laser-direct-drive research to characterize the imploding target [34]. With LDD one also has access to unobstructed, multiple-view X-ray and particle-based (neutrons and charged particles) diagnostics that enable 3-D reconstruction of the imploded target, which can then be compared to 3-D simulations [34,35]. In addition, unique to LDD, the hot, multi-keV temperature plasma corona can serve as a radiation source to backlight the imploding target from multiple directions [36]. This interplay between experiments and simulations is required to advance the understanding of target performance and to eventually demonstrate laboratory fusion. As computing capability continues to grow, enabling 3-D simulations [37] with improved physics models, experiments and diagnostics must also improve. Multiple line-of-sight diagnostics (X-ray and neutron imaging, areal density, ion temperature, etc.) cross-calibrated and timed to provide 3-D information for comparison with modeling are essential and should be pursued.

### 2.2. Direct-drive challenges

Even with all of these positive features, laser direct drive must successfully address significant challenges to realize its fusion potential. As with laser indirect drive, LPI remains a major issue for laser direct drive. Fig. 5 schematically shows the processes that occur in the underdense corona of a laser-driven target as a function of the radius. The dependence of the gain on the plasma conditions demonstrates the need to (1) conduct experiments at relevant conditions and (2) accurately characterize the plasma.

As discussed above, overlapped beams, even though individually at below threshold intensities, can act cooperatively to drive LPI [28]. As mentioned in Sec. 2.1, the main LPI challenges are CBET, $2\omega_{pe}$, and SRS. Minimizing the energetic electrons produced by SRS and $2\omega_{pe}$ is critical for laser direct drive given the thin shells caused by the relatively low electron-driven mass ablation rate and the close proximity of the plasma where the interaction physics take place to the fuel, which is to be kept at a low adiabat. Simulations for direct-drive designs that achieve gain show that only small levels (~0.1% of the laser energy) of energetic ($T_{hot}$ ~ 40−60 keV) electrons produced by $2\omega_{pe}$ and SRS can be tolerated before the implosion adiabat is compromised by electron preheat [24]. All of these instabilities depend on the laser intensity, which in turn is key to determine the ablation pressure.

Ignition and gain direct-drive targets at MJ laser energies such as the NIF will be nominally 4× larger than those used on the ~30-kJ OMEGA laser $((R_{NIF}/R_{\Omega}) \sim (E_{NIF}/E_{\Omega})^{1/3})$ [24]. The single-beam intensity threshold for the instabilities depends on the plasma conditions and is reduced with larger plasmas generally scaling inversely with plasma scale length (Eq. (3)). In contrast, the LPI linear gain generally scales with the plasma size. Understanding the limits in laser intensity under ignition-relevant plasma conditions is a key element in the laser-direct-drive program.

Since the major advantage of direct drive is the increased driver-target coupling, CBET schematically shown in Fig. 6 is at present the main LPI concern for direct drive. CBET as mentioned above is essentially seeded Brillouin scattering, which occurs with beams of similar or equal frequencies since the ion-acoustic frequency $\omega_{iaw}$ is much less than the laser frequency [25]. As shown in Fig. 6(b), CBET not only reduces the target absorption, but since it "robs the beam energy" from reaching the highest plasma densities, the ablation pressure is even further reduced. Given the dispersion relationship for ion-acoustic waves

$$\omega_{iaw} = k_{iaw} c_s + k_{iaw} \cdot v_{flow}. \quad (4)$$

CBET occurs near the Mach-1 surface $(c_s/v_{flow} = 1)$ in the corona at densities $< n_c/4$ for beams with identical

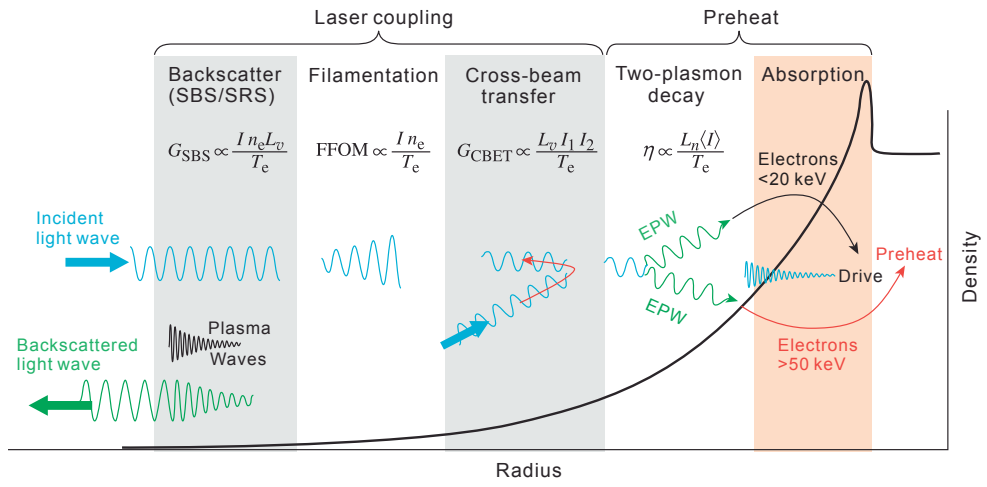


Fig. 5. Laser–plasma processes in the underdense plasma corona. Inverse bremsstrahlung (proportional to $(n_e)^2$) absorption occurs up to $n_c$.

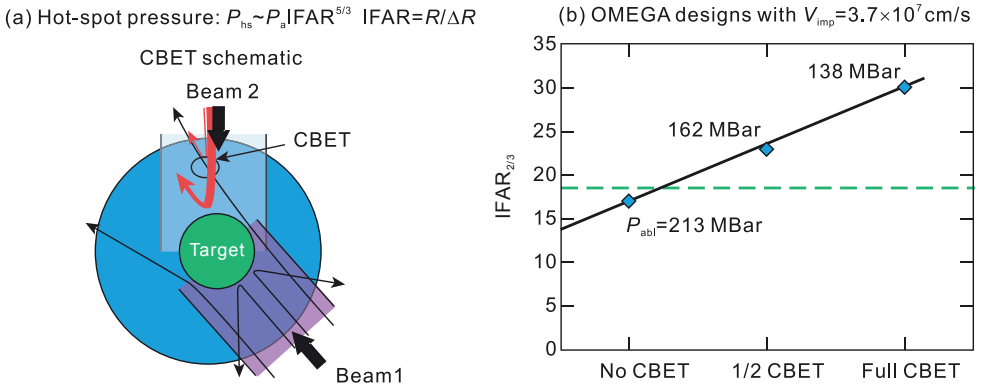


Fig. 6. (a) Schematic of CBET and (b) the impact on required shell in-flight aspect ratio (IFAR) to achieve the implosion velocity required for ignition.

frequencies such as the present OMEGA laser [14]. Despite the low individual beam intensity and the radial flow velocity gradient that both lead to small gains, the EM seed provided by reflected or refracted light, CBET can lead to significant energy and ablation pressure loss. For example, present OMEGA implosion experiments are best matched when 10%–20% of the laser energy is lost because of CBET [24].

It is straightforward to show that the hot-spot pressure is directly related to the ablation pressure and in-flight aspect ratio (IFAR) of the imploding target, where IFAR is the ratio of the shell radius to shell thickness and is a key metric for the hydrodynamic stability of the implosion [2–4,24]

$$P_{hs} \sim P_{abl}\text{IFAR}^{5/3}. \quad (5)$$

If CBET reduces the ablation pressure (see Fig. 6(b)), thinner, less-stable shells must be imploded to achieve the needed implosion velocity to achieve the ignition hot-spot pressure $P_{hs}$ $\sim(v_{imp})^{10/3}$ with the reduced mass of the target. Modeling and simulations show that stable implosions require that the shell IFAR at maximum acceleration be limited to values of the order of 20 [3,24]. It is clearly important for laser direct drive to not only minimize CBET but also to understand its impact on symmetry and hot-electron generation. As discussed below, when CBET is reduced, higher laser intensity will occur at densities ($0.15\ n_c < n_e < 0.25\ n_c$) where instabilities occur that can produce energetic electrons; this must be understood and addressed too.

In addition to CBET, $2\omega_{pe}$, and SRS instabilities [25] remain an issue for laser direct drive. The effective temperature of electrons generated by these instabilities can be 40 keV–100 keV and can have sufficient range $\sim(E_e)^{1.2}$ [2] to readily preheat the fuel and raise the adiabat. Since the waves must satisfy the plasma dispersion relationships, phase matching, and energy conservation, these instabilities occur near $n_c/4$ for $2\omega_{pe}$ and at $n_e < \sim n_c/4$ for SRS. For OMEGA cryogenic implosion experiments with a peak summed intensity of $\sim10^{15}$ W/cm$^2$, the plasma corona conditions at $n_c/4$ are ~2.8 keV at a scale length (limited by the capsule size) of ~150 μm [38]. In these experiments, supported by both modeling and data (the threshold for SRS backscatter is $\sim7.5 \times 10^{15}$ W/cm$^2$), the dominant source of hot electrons is the two-plasmon–decay instability with levels <1% of the incident laser energy [39]. Experiments have also shown that the hot-electron source produced by this instability at $\sim n_c/4$ appears to be isotropically emitted in the forward $2\pi$ direction [40]. Since the radius of the $n_c/4$ surface is nominally twice as

large as that of the cold fuel, the number of energetic electrons that preheat the fuel will be less than those created by the instability. These experiments also show the importance of understanding the transport and source characteristics of the hot electrons.

As previously discussed, one feature of laser direct drive is that the intensity in the corona is the sum of the individual overlapped beams rather than that of a single beam. Modeling $2\omega_{pe}$ instability (and LPI issues in general) must take this into account. An analysis of $2\omega_{pe}$ experiments on OMEGA employing both planar and spherical targets clearly shows "multibeam effects"; it also shows that the instability levels (threshold and saturation) depend on the polarization of the beams and the laser beam and target geometries [28,29,39]. These experimental results are best modeled when a common-wave gain $G_c$ scales as $I_\Sigma L_n \lambda_L / T_e$, where $I_\Sigma$ is the summed intensity (at $n_c/4$) of the individual beams that share a common electron plasma daughter wave; the other parameters have been defined previously. Since the gain depends on the electron density scale length $L_n$, this instability remains an issue for the larger ignition/gain direct-drive targets.

Multibeam effects can also impact the physics of SRS. In a similar fashion to the $2\omega_{pe}$ instability, when beams share a common electron plasma daughter wave, the beams can act together to drive SRS. Of particular concern is the possibility that overlapped beams propagating in an inhomogeneous corona can drive SRS collectively as an absolute instability (growing exponentially in time) at densities far below $n_c/4$, where SRS is normally convective [25,30]. When this occurs, the intensity threshold can be significantly less than the overlapped beam intensities for ignition LDD (~$10^{15}$ W/cm$^2$) and for convective SRS at $n_e < n_c/4$. Again, the physics will depend on the details of the beam-target geometry including the polarization strategy. Analysis indicates, albeit with several simplifying assumptions, that the overlapped intensity threshold scales with the local plasma scale length as $(L_n)^{-4/3}$. As mentioned previously, SRS has historically been the dominant hot-electron source in the large plasmas in hohlraums employed in laser indirect drive [4]. With the larger coronas at ignition scale, this process may become important for direct drive. Understanding and controlling LPI in MJ-ignition-scale plasmas with the complexity of multiple overlapped beams is clearly a critical area of research for laser direct drive (and all laser approaches). If SRS is indeed absolute it can more easily be reduced by multi-THz laser bandwidth. NRL and LLE are exploring means that may enable such bandwidths with existing lasers.

In addition to laser–plasma interaction physics, challenges associated with the hydrodynamic performance of laser-direct-drive targets must also be addressed. While the principal advantage of laser direct drive is the increased mass that can be imploded as a result of the direct coupling of the laser to the target, the direct illumination of the target presents additional challenges to the quality of the laser, target placement, and fabrication. In addition, as in laser indirect drive, one must consider the role of "engineering features" such as fill tubes or mounting stalks or tents in overall target performance. Such features have been shown to impact LID target performance in NIF experiments [37]. It should be expected that these inherently 3-D features would also impact target performance for laser direct drive.

When evaluating the hydrodynamic behavior of ICF implosions, it is useful to differentiate the physics using the product of $k\Delta$, where $k$ is the wave number of the instability and $\Delta$ is the shell thickness of the imploding target at maximum acceleration [4,24]. The reason for this is that the initial "noise" sources arise from very different seeds and their evolution and impact on target performance can be very different. For example, the sources for low modes with laser direct drive (modes with long wavelength given by $k\Delta < 1$, where the mode number $\ell = kR$) are laser power imbalance, beam pointing, overall beam geometry arising from a finite number of beams, target placement, and any large-scale nonuniformity in the thickness of the cryogenic fuel or ablator. These low modes generally grow secularly in time and can be enhanced by the Rayleigh–Taylor (RT) instability and Bell–Plesset growth during deceleration at the final stages of the implosion [24]. For X-ray drive the low modes are also influenced by beam placement, hohlraum geometry, case-to-capsule ratio, hohlraum wall albedo, and laser-energy deposition in the hohlraum plasma [4]. For both direct and indirect laser drive, several of these parameters are also time dependent [4,24].

In contrast, the noise sources for the short-wavelength modes ($k\Delta > 1$) are high-spatial-frequency intensity nonuniformities ("speckle") caused by the relatively high coherence of the laser, high-spatial-frequency nonuniformities in the fuel layer or ablator, and small defects and/or surface particulates that are formed or accumulate during the fabrication, fueling, or fielding of the target. It is important to recognize that fueling and fielding targets for experiments can also result in "seeds" for the RT instability even with a perfectly uniform ablator, particularly when permeation filling is used to "fuel the targets" [24]. The long time required to fill the targets with DT by permeation plus the β decay of the tritium can result in radiation damage and charging of the target that can lead to the accumulation of submicron features on the target surface.

Both LID and LDD central hot-spot ignition ICF targets are hydrodynamically unstable at two phases of the implosion: during acceleration at the ablation surface and stagnation at the inner shell surface with the RT instability exponentially amplifying these high-spatial-frequency noise sources. The RT instability occurs at the interface between a light and a dense fluid. The interface is RT unstable when the pressure and density gradients have opposite signs (when $\nabla\rho \cdot \nabla\rho < 0$) [41] with a classical exponential growth rate ~$(ka)^{1/2}$, where $k$ as mentioned above is the wave number of the perturbation and $a$ is the acceleration at the interface. While the Richtmyer–Meshkov (RM) instability can serve to enhance the noise source for RT at a shocked interface and Kevin–Helmholtz (KH) can influence the late-time nonlinear evolution of the "bubble and spikes" from RT, addressing this instability is a major challenge for both laser direct and indirect ICF [1–4].

Even with the relatively large mass (~mg) of the imploded fuel for direct drive for MJ-class laser drivers, convergences $C$ of ~20–22 are still necessary to achieve the pressures required for fusion [24]. The absorbed laser intensity must be very uniform since an implosion will amplify any nonuniformity in implosion velocity ($v_{\rm imp} \sim I^{1/3}$) or ablation pressure ($P_{\rm abl} \sim I^{2/3}$) in the final fuel assembly. Any variation in these quantities must therefore be minimized (i.e., $\delta v_{\rm imp}/v_{\rm imp} \sim (C-1)^{-1}$). To achieve the required convergence, simple estimates and 3-D simulations show that the overlapped intensity on the target must be balanced to a few-percent root mean square (rms) [2,3,24]. Simulations for hydrodynamically scaled ignition/gain targets on the 60-beam OMEGA laser show that this balance is required so that the low-$\ell$ modes ($\ell < 10$) do not significantly impact the implosion's performance. As mentioned above, this requirement places demands on laser power balance, beam pointing, and target placement in addition to target fabrication. If imbalance in these low modes is present and they grow during stagnation then 1-D implosion performance is compromised. The presence of these modes can lead to an increase in hot-spot volume and a reduction in pressure, create thin regions in the cold shell that can reduce confinement and reduce the conversion of kinetic energy into internal energy at stagnation. Degradation in implosion performance has been observed for both direct- and X-ray–driven targets irradiated on both the NIF [27] and OMEGA [24] and is attributed to the presence of these low-mode asymmetries. These experiments show yields and areal densities that are lower than 1-D calculations. Imaging (X-rays and neutrons on the NIF and X-rays on OMEGA) shows deviations from "roundness" and time-of-flight fusion neutron measurements from multiple directions indicate a significant fraction of the implosion energy is not converted into fuel internal energy at stagnation. As mentioned above, whereas in laser indirect drive, the majority of the low-mode asymmetry ($\ell = 2, 4$) is caused by the laser deposition in the hohlraum and the finite case-to-capsule ratio of the target; in direct drive the asymmetries arise from all of the factors listed above.

In addition to the long-wavelength nonuniformity, the impact of short-wavelength modes ($k\Delta > 1$) is a major concern for laser direct drive. During acceleration the instabilities at the ablation surface can break up the shell in flight or feed through (RT instabilities are surface waves decaying exponentially ($\sim e^{-k\Delta r}$) from the unstable interface) to the inner ice surface and provide additional noise sources when the hot spot is decelerating the shell at stagnation. This can lead to a mix of cold fuel or ablator into the hot spot and higher thermal conduction losses thereby preventing ignition. RT-driven high spatial instabilities are more challenging for direct drive than X-ray drive for several reasons: there are additional "noise sources" and as discussed below, the RT growth rate is higher because ablation in laser direct drive is driven by electron conduction [1–4].

In contrast to X-ray drive where thermal X-rays ($T_{\rm rad}$ ~ 250–300 eV) from the laser-heated hohlraum drive the capsule, direct drive must address high-spatial-frequency noise sources initiated by the laser drive. Early in the development of ICF, the poor quality of individual laser beams arising from phase aberrations and the high degree of coherence was a major concern and limitation for laser direct drive. For example, at the focus of the laser with wavelength $\lambda$, high-frequency variations (speckles) in the laser intensity with transverse dimensions $d_{\rm spec} \sim f^{\#}\lambda$ ($f^{\#}$ is the $f$ number of the lens) occur with the peak intensity many times (>4×) that of the average. Since the mass ablation rate and ablation pressure depend on laser intensity ($\delta m/\delta t \sim I^{1/3}$ and $\delta p/p \sim I^{2/3}$), any variation in intensity will lead to mass perturbations of the target that then act as seeds for hydrodynamic instabilities. Even with overlapped beams, this is particularly damaging early in the laser pulse, when the distance between where absorption takes place (at $n_{\rm e} \sim n_{\rm c}$) and the ablation surface is minimal. Thermal conduction is ineffective in reducing the nonuniformities [2,3,24] when the "smoothing" distance is small and is made more difficult with shorter-wavelength lasers with the critical density scaling as $(\lambda)^{-2}$.

The laser-direct-drive community has made significant progress in addressing this issue by inventing a variety of "beam-conditioning" techniques such as distributed phase plates (DPP's) [42] induced spatial incoherence (ISI) [43], smoothing by spectral dispersion (SSD) [44], and polarization smoothing [45]. Both ISI and SSD vary the on-target intensity in time but at a frequency limited by the gain bandwidth ($\Delta\nu$ ~ THz) of the laser media or the nonlinear frequency up-conversion crystals when solid-state lasers are the driver. The rate at which the intensity nonuniformity decreases to its asymptotic level increases as $(\Delta\nu)^{-1}$, so larger-bandwidth drivers will always be desired. Despite the improvements in the on-target intensity, demonstrating that imprint will not be an issue for ignition/gain laser-direct-drive targets is a component of the laser-direct-drive research program. In order to accomplish this task, a strategy for imprint reduction should best be viewed as a "system issue" that includes target design, irradiation strategy, and laser modifications.

It is important to recognize that beam smoothing is also important for laser indirect drive even though it is not an issue directly related to capsule hydrodynamics [25,31]. While present lasers do not have sufficient bandwidth to directly influence the high-frequency LPI processes (the bandwidth must be comparable to the inverse growth rate of the instability ($\Delta\nu$ ~ 10 THz) [25,28,31]), it is adequate to suppress filamentation. Filamentation increases the local laser intensity and can then lead to instabilities, such as SRS, SBS, and $2\omega_{\rm pe}$, and beam steering. Beam conditioning should be a feature for all laser drivers regardless of the target approach (laser indirect drive, MagLIF).

In addition to the additional noise sources for LDD as mentioned above, the growth rate of the RT instability is higher than that for LID [2–4]. Modeling and simulations of RT show that when ablation and a finite density gradient at the interface are present, the classical RT growth rate $\gamma$ is modified to [2–4,24]

$$\gamma = \sqrt{ka/(1+kL)} - \beta k v_{\rm abl}, \tag{6}$$

where $k$ (the perturbation wave number) and $a$ (the acceleration) have been defined previously, $L$ is the density scale

length at the interface, $v_{abl}$ is the ablation velocity ($v_{abl} = (\delta m/\delta t)/\rho$), and $\beta$ is ~1.5−3, depending on the ablator material [2−4]. The stabilizing term from ablation and the reduced growth arising from the density scale length because RT modes are surface waves. Since the ablation in LDD is driven by electron conduction rather than thermal X-rays, the density scale length at the ablation surface is of the order of the electron mean free path (~few microns). When the ablator is CH as the nominal case, radiation from the hot corona will also increase the density scale length somewhat but it will still be smaller than laser indirect drive. In addition, electron-driven mass ablation rate and therefore the ablation-front velocity is less than that of X-ray drive with values typically ~10% of that from LID [2−4]. The RT instability will grow exponentially until the perturbation amplitude is of the order of the wavelength of the mode; then the width of the multi-mode mix region will grow proportional to $at^2$. As a result, the modes with $k \sim 2\pi/\Delta R$ that can break up the shell in flight are the most dangerous.

To increase the ablation velocity, laser-direct-drive targets generally employ adiabat shaping [2,3,46], where the adiabat $\alpha$ at the ablation surface is raised, thereby lowering the density and raising the ablation velocity ($v_{abl} \sim \alpha^{3/5}$). The adiabat of the main fuel is kept low so that high gain is still possible. Adiabat shaping is done by shaping the laser drive (Fig. 4), where a short-pulse "picket" pulse first irradiates the target before the main pulse, launching a shock that then decays as it propagates through the shell, raising the adiabat at the ablation surface and leaving the main fuel at an acceptably low value. In laser direct drive with adiabat shaping, the ablation velocity can become comparable to thermal X-ray−driven ablation.

In addition to laser−plasma interaction physics, a quantitative understanding of the implosion hydrodynamics for ignition/gain target designs is therefore critical to realizing the potential of laser direct drive. A research program that explores and determines the dependence and sensitivity of the performance on both low-mode nonuniformities and the RT instability is an essential component of the national laser-direct-drive program.

With this background, the laser-direct-drive program that addresses both LPI and hydrodynamics issues for laser direct drive utilizing both OMEGA and the NIF will be described.

## 3. LDD research plans on OMEGA and the National Ignition Facility

### 3.1. Strategy

Motivated by the above challenges, a laser-direct-drive strategy has been established whose goal over approximately the next five years is to explore and demonstrate a quantitative understanding of the physics required to achieve fusion ignition and gain at MJ-scale laser energies with direct drive with a facility such as the NIF. This strategy involves multiple facilities and institutions, consistent with the physics goals of the program. All of these elements must be successfully completed before any significant modifications to the NIF for laser direct drive are to be made (e.g., reconfiguring the illumination geometry for spherical direct drive).

The elements of the direct-drive program include the following:

1. The experimental demonstration on the 60-beam OMEGA laser of ignition-relevant hot-spot pressures for direct-drive implosions at MJ-scale laser energies available on NIF. A quantitative understanding of the coupling, implosion, and stagnation physics of hydrodynamically scaled cryogenic targets is required to achieve this goal. Achieving inferred hot-spot pressures of the order of 100 Gbar and understanding the sensitivity of the implosion to laser performance (on-target power, beam quality, and intensity balance), target-beam placement, target quality, and engineering details (such as target fill tubes and mounting structures) are also goals of the program.
2. An understanding and demonstration of acceptable laser−plasma interaction and target-coupling physics (laser-target absorption, electron transport, and imprint mitigation), CBET, and preheat sources (electrons from $2\omega_{pe}$ and SRS and penetrating X-rays from the target corona) at the MJ-scale laser energy on the NIF. As mentioned above, a major positive feature of the LDD program is the ability to explore the coupling physics at the ignition-scale plasma conditions on the NIF. As mentioned above and as experience has shown over multiple decades, quantitative scaling of LPI with increasing driver energies, multibeam irradiations and resulting plasma conditions has not been possible. Incorporating accurate "first-principle" physics models into multi-dimensional radiation−hydrodynamic codes is extremely challenging because of the spatial and temporal scales of the important physics and the complex nonlinear physics of LPI.
3. Evaluation of the cost, schedule, and impact of converting the NIF for spherical direct-drive irradiation. During the reviews that led to the approval of NIF, the possibility of exploring direct-drive target concepts was extensively discussed. At that time, it was concluded that insufficient data existed to make spherical-illumination laser direct drive the NIF baseline. Recognizing the advantages of LDD as discussed above, the Department of Energy instructed the NIF "not to preclude direct drive." As a result, laser ports for spherical illumination were made in the NIF target chamber. Studies are underway to explore the impact of moving the beams and improving the beam conditioning of the NIF for direct drive. The OMEGA and NIF research program described below will further define the requirements for direct drive on the NIF.
4. Robust symmetric direct-drive alpha heating, low-gain ($G \sim 1$) and high-gain ($G > 10$) designs. LDD targets that achieve high gain are the end—not the first—goal of the ICF ignition program. High-gain targets with MJ-class drivers place extremely challenging requirements on the physics, driver precision, and target fabrication. Over the next several years, as the physics of "ignition" are further developed, direct-drive target designs that are focused on

alpha heating and low gain will be active areas of research. The high-foot LID designs that demonstrated alpha heating are successful examples of this approach [8]. Recent experiments on OMEGA, when scaled to NIF energies, were calculated to provide similar levels of alpha heating provided that the coupling physics and scaled implosion core conditions are reproduced on the NIF. The yields of such direct-drive implosions at the NIF scale would result in ~125 kJ of fusion, showing the advantages of imploding more fuel mass made possible by the increased driver coupling [47].

### *3.2. 100-Gbar hydro-equivalent implosion program on OMEGA*

As shown in Fig. 3, fuel pressures in the range of 120–140 Gbar with fuel convergence of ~22–24 are required for ignition if 30–40 kJ of energy is coupled to the hot spot. Such energies are potentially available on the NIF if properly configured for direct drive and, as discussed in Sec. 2.2, laser–plasma instabilities such as CBET are minimized or eliminated. Hot-electron preheat from either SRS or $2\omega_{pe}$ must also be acceptable and will play a key role in determining what fuel adiabat can be achieved in the implosion. An important success of the LID research on the NIF, as previously mentioned, is the inference of ~230-Gbar pressures on the NIF in X-ray–driven targets, demonstrating that the pressures needed for robust ignition with direct drive have been achieved in a laboratory implosion system [8,27].

Cryogenic implosion experiments on OMEGA are hydrodynamically scaled from ignition/gain designs that could be irradiated on the NIF. Displayed in Fig. 4, the target size and irradiation pulse scale as $(E_L)^{1/3}$ and the laser power as $(E_L)^{2/3}$, while the target mass scales directly with the absorbed energy. In these scaled targets, the peak laser intensity, implosion velocity, adiabat, IFAR, and hydrodynamic instability growth factors are identical to MJ designs. In order to address the physics and to provide the community with a readily communicated goal, the national LDD program has established the achievement of a 100-Gbar hot-spot pressure as a major objective [24]. It is important to understand that for this element of the LDD program to be successful, achieving the fuel pressure is not sufficient. Simulations that contain the important physics must match all of the experimental observables. An understanding of the "robustness" of the target's performance and the dependency on and sensitivity to input conditions (laser performance, target quality, etc.) are also a critical component of the program. Achieving such pressures on the ~30-kJ OMEGA laser is more hydrodynamically challenging than on the NIF given smaller targets. For example, 3-D effects should have more impact on the quarter-scale OMEGA targets and thermal losses should be greater given the larger surface/volume ratio ($\sim R^{-1}$) of the OMEGA targets (in an idealized 1-D implosion, simple estimates using Spitzer conductivity give $T_i$ scaling as $R^{2/7}$; deviations from a 1-D implosion would almost certainly increase conduction losses). The impact of engineering features such as fill tubes required to fuel the target or mounting stalks would be expected to be larger for these smaller targets. As mentioned above the mounting tent used to place capsules in hohlraums for LID experiments on NIF have been shown to seed the RT instability [37].

Even though this implosion goal is below that required for ignition at present NIF energies, the achievement of a well-modeled and well-understood 100-Gbar hot-spot pressure on OMEGA would be a major milestone for the LDD program. Although significant research remains to be done, it appears to be an achievable multiyear goal if improvements are made to the OMEGA laser, targets, and diagnostics, and if the program continues to refine and improve the physics understanding—a goal of the 1-D campaign discussed below. It would give the ICF community confidence that hydrodynamic performance of direct drive would lead to ignition at NIF-scale energies. In addition, achieving a hot-spot pressure of 100 Gbar on the NIF would also lead to significant fusion yields. Estimating the total fusion yield (hot spot and surrounding cold fuel) including alpha heating using the no-alpha Lawson parameter $\chi_{no\ \alpha}$ analysis of Betti et al. and extrapolating to NIF energies ($\chi_{no\ \alpha} \sim E^{0.35}$) would give a yield in excess of a megajoule [47,48]. The enhancement of the yield resulting from alpha heating would be $>10\times$ that arising from the implosion $p\delta V$ work alone.

Cryogenic experiments on OMEGA to date have achieved peak inferred pressures of ~56 Gbar with ~0.440 kJ coupled to the fuel out of an incident laser energy of 26 kJ [49]. These pressures are inferred by neutron measurements (yield, ion temperature, burn duration) and X-ray imaging of the hot spot by the following equation:

$$P_{hs} = \left( 32Y\sqrt{\ln 2/\pi} \Big/ \left\{ \Delta t_{burn} \int\limits_{V_{hs}} \delta V \left[ (\sigma v)/T^2 \right] \right\} \right)^{1/2}, \quad (7)$$

where $Y$ is the fusion yield, $\Delta t_{burn}$ is the burnwidth, $\sigma v$ is the burn rate, and $T$ is the ion temperature. The integral is over the hot-spot volume with a radial dependence of temperature suggested by both simulations and analytical models.

While these are impressive results, comparable to the high-foot NIF LID results when hydrodynamically scaled to NIF energies (assuming no LPI degradation in the coupling physics), they are not sufficient to give confidence that LDD can achieve ignition on the NIF. For example, the ideal 1-D performance of these OMEGA targets would result in inferred pressures approaching 90 Gbar [49].

A summary of the cryogenic implosion experiments on OMEGA is shown in Fig. 7 [24]. The figure shows the OMEGA results: 1-D calculated hot-spot pressure normalized to the threshold pressure $P_{th} = 250\ \text{Gbar}\ (E_{hs}/10\ \text{kJ})^{-1/2}$ for ignition and scaled to NIF energies (Fig. 3)

$$P_{scaled} = P^{\Omega}/P_{th} \quad (8)$$

as a function of fuel adiabat. $P_{scaled}$ equal to 1 implies hot-spot ignition. The plot also shows 1-D simulations with and without

CBET. The simulations suggest that if CBET can be eliminated, ignition could be achieved at NIF-scale energies, even at fuel adiabats of ~5. This result again shows the need to address CBET for laser direct drive.

While the reasons for the degradation in performance in hot-spot pressure are not fully understood, extensive analysis of the cryogenic target experiments and 2-D and 3-D modeling strongly suggests that power balance, target offset from chamber center, and cryogenic target quality are the limiting factors [24,47,49]. As discussed in Sec. 2.2, these experimental limitations (power balance and target offset) lead to the breakup of the shell, reduce the peak pressure, and truncate the fusion burn. In addition, these low-adiabat implosions also suffer from ablator mix into the hot spot caused by high-mode instabilities resulting from seeds resulting from target quality at "shot time" or laser imprint. The overall result is a reduction in pressure, burn duration, areal density, peak ion temperature, and fusion yield. In addition, these experiments at overlapped intensities of $\sim 8 \times 10^{14}$ W/cm$^2$ show strong evidence for CBET. As discussed above, CBET reduces the target absorption (and perhaps increases drive nonuniformities), resulting in the need for thinner shells to achieve the required implosion velocities, further exacerbating hydrodynamic instabilities. While not as dominant a factor in performance as power balance, off-center positioning, target quality, laser imprint, and CBET, the hot electrons produced by the $2\omega_{pe}$ instability may also be impacting target performance by raising the shell adiabat.

Given the challenges and to provide benchmarks for understanding, the laser-direct-drive program has adopted a phased approach where the goal is a well-understood implosion that first achieves a less-demanding pressure of 80 Gbar. Modeling and simulations indicate that this goal can be achieved with improvements to the present Omega Laser Facility and target fabrication. For example, 2-D and 3-D simulations indicate that this inferred pressure can be achieved with cryogenic targets with CH ablators if the OMEGA laser power balance is ~3% rms (sampled over 100 ps), and the target is placed at the chamber center within ~10 μm (the hot-spot radius is of the order of 20 μm). Improved target coupling

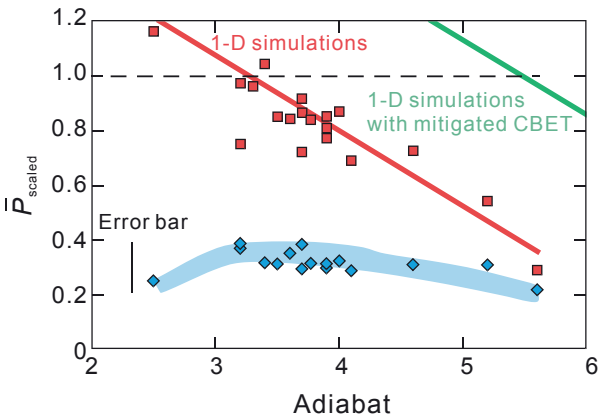


Fig. 7. Normalized hot-spot pressure scaled to NIF energies as a function of adiabat. Inferred pressures from OMEGA cryogenic experiments are plotted as well as 1-D simulations with and without CBET losses.

(i.e., reduced impact of CBET) that enables implosions with IFAR's that should enable adequate hydro-stability can be achieved by slightly reducing the individual laser beam diameter relative to the target diameter. This reduces the implosion symmetry somewhat but is believed to be acceptable for this intermediate goal.

To achieve the 100-Gbar goal, further improvements in the laser power balance ($\Delta P_{rms}$ ~ 1%) and target positioning ($\Delta r_{pos}$ ~ 5 μm) are thought to be required based on 3-D simulations [24,50]. In addition, CBET must be significantly reduced so that thicker, more hydrodynamically stable shells (lower IFAR) can be imploded. Several options are presently being explored including modifying OMEGA to have several incident laser wavelengths to "move the CBET resonance" (Eq. (4)) to lower densities with less SBS gain and reducing the laser spot during the pulse. This latter approach, referred to as "zooming" by the ICF community [2,3], should be a feature in any future laser that is focused on the direct-drive target approach. Research over the next several years will determine the optimal solution that will include understanding the impact on hot-electron generation, implosion symmetry, and imprint. A particular concern for the 100-Gbar goal is that by reducing CBET, higher-intensity light will reach $\sim n_c/4$, where hot-electron production by the $2\omega_{pe}$ occurs. Since this instability gain scales as $(T_e)^{-1}$, present designs have a higher-$Z$ thin (i.e., silicon) layer placed in the ablator so that at peak intensity a higher-$Z$ and hotter corona exist at $\sim n_c/4$.

As discussed earlier, laser direct drive is susceptible to the RT instability seeded by high-spatial-frequency noise sources. To achieve both pressure goals, reductions in the noise sources from surface debris, nonuniformities in the ablator or ice layer, or laser imprint are required. Target characterization with appropriate resolution (~0.5 μm) as close as possible to "shot time" is clearly needed as well as a more detailed understanding of imprint.

It is important to recognize that these goals require a detailed physics understanding of laser–plasma interactions, equation of state, energy transport, and hydrodynamics. The present limitations of the Omega Laser Facility, target fabrication, and diagnostics and their impact on target performance can mask a lack of understanding of the underlying physics. This would be particularly true for low-adiabat implosions with high convergence and demanding hydrodynamic stability. For these reasons a critical element of the 100-Gbar Program is the "1-D Campaign," whose goal is to understand and model implosions with high adiabat ($\alpha$ ~ 7) and low convergence (<15), where the sensitivities to laser performance, preheat, and hydrodynamic instabilities are minimized. Demonstrating 1-D performance and scaling (i.e., $P_{abl}$ and IFAR, respectively) given, for example, by Eq. (9) is a goal of this campaign with a self-consistent set of experimental observables:

$$P_{1\text{-D}}^{hs} \sim P_{abl}\text{IFAR}^{5/3},$$
$$E_{1\text{-D}}^{hs} \sim E^{kin}\text{IFAR}^{2/3}. \quad (9)$$

If the laser-direct-drive program can achieve and have a robust understanding of ~100-Gbar implosions on OMEGA, a

compelling case that ignition can be achieved on the NIF configured for spherical illumination can be made provided LPI is acceptable and the NIF laser can achieve the necessary precision. A robust understanding of the 100-Gbar implosions includes not only the ability to model success but to understand and model failure.

### *3.3. MJ laser−target coupling program on the NIF*

As has been discussed previously, a critical feature of the laser-direct-drive program that was not available for the indirect-drive program prior to the NIF planning and construction is the presence of a MJ laser facility where laser−plasma interaction physics can be explored at ignition-scale energy. Fig. 5 lists the interaction processes that occur in the underdense corona and whose scaling and levels must be measured and understood.

Even though the NIF is presently configured for indirect drive and does not have optimal beam smoothing and the diagnostic configuration for irradiating hohlraums, significant progress in understanding and exploring LPI mitigation strategies for LDD is possible. The diagnostic limitation is primarily related to optical scattered light, limiting the ability to infer global energy coupling. These diagnostics however should be readily modified/added for direct-drive research on the NIF. In addition planned diagnostics such as deep UV (~0.2-μm) Thomson scattering will enable plasma characterization at relevant densities $(n_c/4)$ as well as directly observing the LPI-produced plasma waves. The majority of X-ray diagnostics (X-ray yield, spectrum, and imaging) including X-ray backlighting developed for indirect drive are appropriate for direct-drive research. NIF also presently has the unique capability for multiple laser wavelengths that enable CBET mitigation strategies to be explored [25,26,28]. The reduced laser conditioning presently available on the NIF (90-GHz, 1-D SSD) and phase plates optimized for irradiating hohlraums [32] will provide "worst-case" scenarios since the improved beam conditioning required for direct-drive, high-performance implosions should have a positive impact on LPI.

Both planar and spherical target platforms are being developed for the MJ LDD Program. Fig. 8 shows the platforms and Table 1 lists the relevant coronal parameters for ignition at the MJ energy scale for direct-drive targets and the conditions that are achievable with the various platforms [51]. The values in Table 1 are shown at $n_c/4$ since this is the density at which hot electrons are produced from $2\omega_{pe}$ and resonant SRS. The corona is also nearly isothermal. As shown in Table 1, plasma and laser conditions very near those expected for direct-drive−ignition designs are possible given the energy and power of the NIF. The table also shows the coronal conditions for OMEGA, with its limited energy and power, that are both smaller and colder. As has been discussed, LPI is very dependent on the plasma conditions so the availability of the NIF eliminates the significant uncertainty in scaling LPI from OMEGA. In addition, the 192 beams of the NIF can be used in various combinations to enable multibeam effects, an essential feature of direct-drive laser-coupling physics to be studied. It is also important to note, that systematic LPI experiments with smaller laser facilities in well-characterized plasmas with sophisticated diagnostics such as Thomson scattering are also important parts of the program. With such experiments, innovative mitigation strategies can be explored and improved physics models developed that can ultimately be tested on the large facilities, where shot rate, diagnostics, and experimental flexibility are more limited.

The MJ Program, summarized in Table 2, has three major campaigns: energy coupling, target adiabat, and laser imprint [51]. The energy-coupling campaign explores CBET and thermal transport (essential for understanding the effectiveness of inverse bremsstrahlung, hydro-efficiency, and thermal smoothing of laser nonuniformities) in ignition-scale plasmas. The multi-wavelength capability of the NIF and the impact on CBET are important features of this program. The adiabat campaign addresses the physics that determine the target adiabat such as shock generation and timing, radiation, and hot-electron production. The imprint campaign explores the impact of beam quality on producing the high-spatial-frequency noise sources that serve as seeds for the RT instability at the ablation surface. All of these campaigns are connected (i.e., reduced CBET can lead to increased levels of $2\omega_{pe}$ and SRS). With each topic as shown in Table 2, the national program is developing mitigation strategies to address issues as they arise [51]. For example, mitigation strategies for LPI (CBET and hot-electron generation) will be explored with wavelength detuning and increasing the electron temperature in the underdense corona. The use of spherical and planar targets also enables one to study multibeam effects with and without CBET on hot-electron production. The NIF also presently has one quad (four beams) with advanced smoothing capability (multi-FM 1-D SSD) [52] developed at LLE, which will be used to study beam-smoothing strategies and the impact on laser imprint. High-$Z$ layers, a technique developed by NRL to create an early-time smoothing plasma prior to laser irradiation will also be explored to mitigate laser imprint [53]. The trade-off between smoothing and radiation preheat can be studied on the NIF given the larger laser energies and thicker targets.

### *3.4. Conversion of the NIF to spherical illumination for laser direct drive*

In the original vision for the NIF was that the facility was to explore all credible approaches to laser-driven ICF over the facility's multi-decadal lifetime. As mentioned earlier, while laser direct drive lacked the database for it to serve as the baseline initial approach, beam ports for spherical illumination of targets were made in the NIF target chamber. Fig. 9 shows the NIF target chamber with the spherical ports prior to placing it in the NIF building. While significant progress has been made since the NIF was constructed, the activities described in Secs. 3.2 and 3.3 must be successful before a compelling case can be made for laser-direct-drive−ignition research on the NIF. Initial direct-drive studies for the NIF focused on the polar-direct-drive approach where the

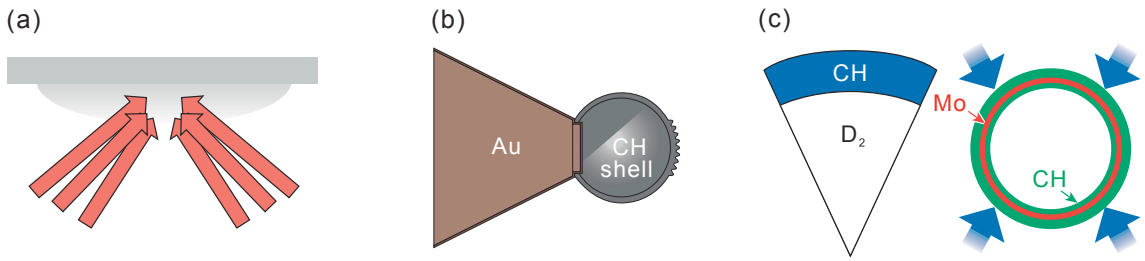


Fig. 8. NIF experimental platforms: (a) planar targets for laser–plasma interaction studies; (b) "cone-in-shell" targets for imprint and coupling studies (planar targets are also used); and (c) implosion targets to study coupling and CBET.

Table 1
Coronal conditions for the MJ LDD Program on NIF and OMEGA experiments.

| Coronal conditions at $n_e/4$ | LDD ignition scale (NIF) | Planar experiments (NIF) | Spherical (implosion) experiments (NIF) | OMEGA Experiments |
|---|---|---|---|---|
| $L_n$ (μm) | 600 | 600 | 300 | 150 |
| $T_e$ (keV) | 5 | 3–5 | ~3.2 | 2.8 |
| $I_L$ (W/cm$^2$) | (5–7) × $10^{14}$ | (5–15) × $10^{14}$ | (5–7) × $10^{14}$ | (5–10) × $10^{14}$ |

Table 2
NIF experimental campaigns.

| MJ campaigns | Physics topics | NIF experimental platforms | Mitigation strategies |
|---|---|---|---|
| Energy coupling | Laser deposition including CBET, thermal transport | Planar and spherical targets, including cone in shell (multi-axis shock timing, scattered light (yield, spectrum), X-ray imaging (self-emission and backlighting) | Wavelength detuning, ablators with high-$Z$ layers |
| Adiabat | LPI ($2\omega_{pe}$, SRS), radiative preheat, shock timing | Planar and spherical targets (multi-axis shock timing, scattered light (yield, spectrum) | Ablators with high-$Z$ layers |
| Imprint | Laser beam conditioning, RT growth | Planar and cone-in-shell targets, X-ray imaging. (self-emission and backlighting) | Multi-FM 1-D SSD, high-$Z$ overcoats |

beam geometry for indirect drive was used [54]. Polar direct drive, shown schematically in Fig. 10, required some of the beams to be repointed and specialized phase plates to be installed on some of the beams to compensate for the reduced equatorial heating of the capsule. Enhanced beam smoothing such as multi-FM SSD would also be required on all of the beams. It has long been recognized that spherical illumination as conducted on OMEGA is the optimal configuration for laser direct drive [1–3]. The NIF has also shown the importance and negative impact of low-order-mode drive

Fig. 9. NIF target chamber prior to installation in the NIF building. The ports for symmetric illumination for direct drive are clearly visible.

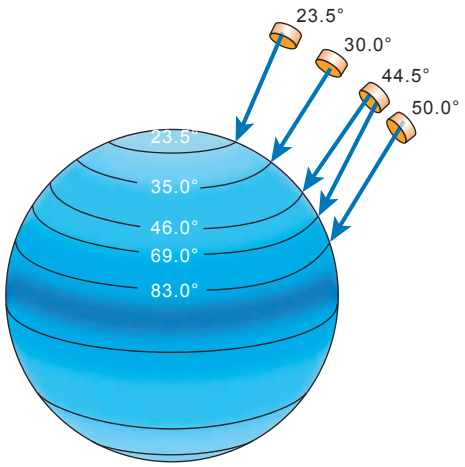


Fig. 10. Polar-direct-drive configuration on the NIF. The figure shows the repointing of some of the NIF beams to improve heating of the equatorial region of the target.

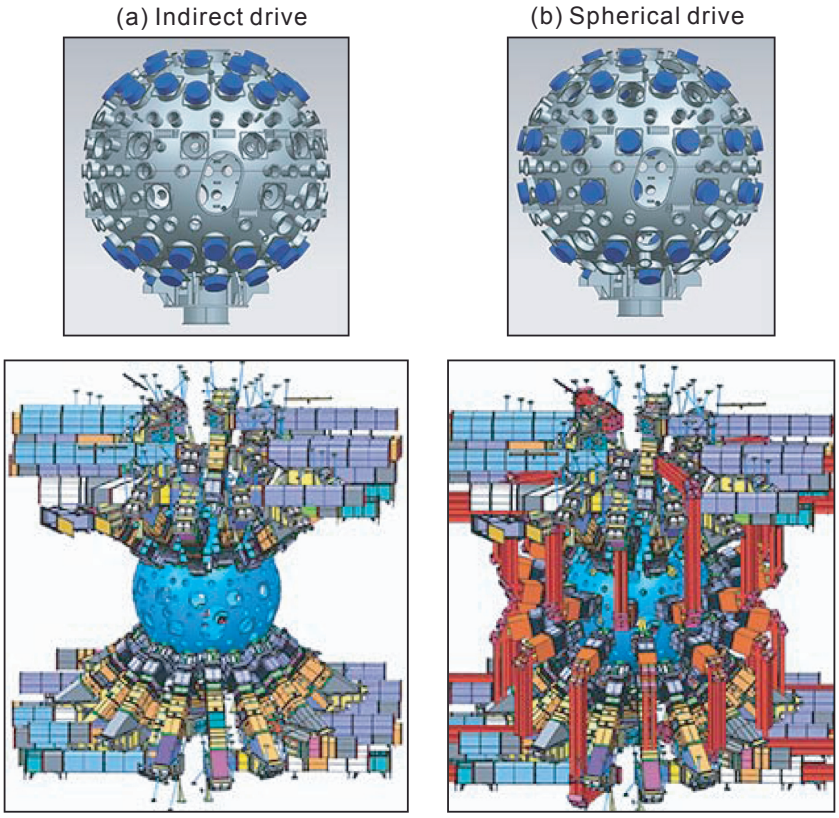


Fig. 11. NIF target chamber beam configurations: (a) indirect drive and (b) spherical direct drive.

asymmetries in implosion performance [32,37]. As a result the present baseline direct drive for the NIF is spherical illumination. Polar direct drive will, however, remain a backup option since the NIF facility impact will certainly be less. Following the successful conclusion of the 100-Gbar Program, research on OMEGA will more fully explore polar direct drive, including capsule modifications such as shimming [55].

LLNL and LLE scientists and engineers have conducted a preliminary investigation of converting the NIF to such a configuration including adding 2-D SSD beam conditioning on all of the NIF beams. The joint study showed that the reconfiguration of the beams, including diagnostic placement, is possible for spherical illumination. An engineering drawing of the beam-path reconfiguration as well as the present illumination configuration is shown in Fig. 11. A final cost and associated schedule for the reconfiguration will require the completion of the research programs on OMEGA and the NIF that will dictate all of the necessary facility requirements and modifications.

### *3.5. Laser-direct-drive target designs*

The achievement of high-fusion-gain target performance remains the long-term goal of the ICF Program. Given the challenges of such implosions, as is now the focus of the laser-indirect-drive program, direct-drive target designs will focus on less-demanding implosions to first understand and demonstrate alpha heating and the onset of ignition. Designing targets over a range of adiabats with reality established by the ongoing research programs on OMEGA and the NIF will be a goal of this effort. Progress in this area, which is in its early phase and involves multiple laboratories, will be reported in future publications.

## 4. Summary

A multiyear coordinated national program to develop laser direct drive is now underway. Over the next years, research at the Omega Laser Facility and the NIF will determine the feasibility and promise of laser direct drive and will eventually lead to an ignition demonstration at the National Ignition Facility, if supported by both the physics and mission. This research will also help guide the design of future drivers and facilities for higher-performance direct-drive fusion.

## Acknowledgment

This material is based upon work supported by the Department of Energy National Nuclear Security Administration under Award Number DE-NA0001944, the University of Rochester, and the New York State Energy Research and Development Authority.

This report was prepared as an account of work sponsored by an agency of the U.S. Government. Neither the U.S. Government nor any agency thereof, nor any of their employees, makes any warranty, express or implied, or assumes

## References

[1] J. Nuckolls, L. Wood, A. Thiessen, G. Zimmerman, Laser compression of matter to super-high densities: thermonuclear (CTR) applications, Nature 239 (1972) 139. http://www.nature.com/nature/journal/v239/n5368/abs/239139a0.html.

[2] S. Atzeni, J. Meyer-ter-Vehn, The Physics of Inertial Fusion: Beam Plasma Interaction, Hydrodynamics, Hot Dense Matter, International Series of Monographs on Physics, Clarendon, Oxford, 2004.

[3] R.S. Craxton, K.S. Anderson, T.R. Boehly, V.N. Goncharov, D.R. Harding, et al., Direct-drive inertial confinement fusion: a review, Phys. Plasmas 22 (2015) 110501. http://scitation.aip.org/content/aip/journal/pop/22/11/10.1063/1.4934714.

[4] J.D. Lindl, Inertial Confinement Fusion: The Quest for Ignition and Energy Gain Using Indirect Drive, Springer-Verlag, New York, 1998.

[5] S.A. Slutz, M.C. Herrmann, R.A. Vesey, A.B. Sefkow, D.B. Sinars, et al., Pulsed-power-driven cylindrical liner implosions of laser preheated fuel magnetized with an axial field, Phys. Plasmas 17 (2010) 056303. http://aip.scitation.org/doi/full/10.1063/1.3333505.

[6] R.M. White, D.A. Resler, S.I. Warshaw, Evaluation of charged-particle reactions for fusion applications, in: S.M. Qaim (Ed.), Nuclear Data for Science and Technology, Springer-Verlag, Berlin, 1991, p. 834.

[7] H.-S. Bosch, G.M. Hale, Improved formulas for fusion cross-sections and thermal reactivities, Nucl. Fusion 32 (1992) 611. http://iopscience.iop.org/0029-5515/32/4/I07.

[8] O.A. Hurricane, D.A. Callahan, D.T. Casey, P.M. Celliers, C. Cerjan, et al., Fuel gain exceeding unity in an inertially confined fusion implosion, Nature 506 (2014) 343. http://www.nature.com/nature/journal/v506/n7488/full/nature13008.html.

[9] A.L. Velikovich, J.L. Giuliani, S.T. Zalesak, Magnetic flux and heat losses by diffusive, convective, and Nernst effects in MagLIF-like plasma, in: 2014 IEEE 41st International Conference on Plasma Sciences (ICOPS) Held with 2014 IEEE International Conference on High-power Particle Beams (BEAMS), IEEE, Washington, DC, 2014.

[10] D.S. Montgomery, B.J. Albright, D.H. Barnak, P.Y. Chang, J.R. Davies, et al., Use of external magnetic fields in hohlraum plasmas to improve laser-coupling, Phys. Plasmas 22 (2015) 010703. http://scitation.aip.org/content/aip/journal/pop/22/1/10.1063/1.4906055.

[11] P.Y. Chang, G. Fiksel, M. Hohenberger, J.P. Knauer, R. Betti, et al., Fusion yield enhancement in magnetized laser-driven implosions, Phys. Rev. Lett. 107 (2011) 035006. http://link.aps.org/doi/10.1103/PhysRevLett.107.035006.

[12] W.J. Hogan, R. Bangerter, G.L. Kulcinski, Energy from inertial fusion, Phys. Today 45 (1992) 42. http://physicstoday.scitation.org/doi/abs/10.1063/1.881319.

[13] E.M. Campbell, W.J. Hogan, The National Ignition Facility—applications for inertial fusion energy and high-energy-density science, Plasma Phys. Control. Fusion 41 (1999) B39. http://iopscience.iop.org/article/10.1088/0741-3335/41/12B/303.

[14] J.M. Soures, R.L. McCrory, C.P. Verdon, A. Babushkin, R.E. Bahr, et al., Direct-drive laser-fusion experiments with the OMEGA, 60-beam, >40-kJ, ultraviolet laser system, Phys. Plasmas 3 (1996) 2108. http://dx.doi.org/10.1063/1.871662.

[15] M.E. Savage, K.R. LeChien, M.R. Lopez, B.S. Stoltzfus, W.A. Stygar, et al., Status of the *Z* pulsed power driver, in: 18th IEEE International Pulsed Power Conference, Omnipress, Piscataway, NJ, 2011, p. 983.

[16] S. Obenschain, S. Bodner, R. Lehmberg, A. Mostovych, C. Pawley, et al., Nike KrF laser development for direct drive laser fusion, in: Plasma Physics and Controlled Nuclear Fusion Research 1990, vol. 3, IAEA, Vienna, 1991, p. 153.

[17] J.T. Hunt, D.R. Speck, Present and future performance of the Nova laser system, Opt. Eng. 28 (1989) 461. http://opticalengineering.spiedigitallibrary.org/article.aspx?articleid=1223525.

[18] 2016 Inertial Confinement Fusion Program Framework, Office of Science and National Nuclear Security Administration, U.S. Department of Energy, Washington, DC, 2016. Report DOE/NA-0044.

[19] M. Tabak, J. Hammer, M.E. Glinsky, W.L. Kruer, S.C. Wilks, et al., Ignition and high gain with ultrapowerful lasers, Phys. Plasmas 1 (1994) 1626. http://dx.doi.org/10.1063/1.870664.

[20] R. Betti, C.D. Zhou, K.S. Anderson, L.J. Perkins, W. Theobald, et al., Shock ignition of thermonuclear fuel with high areal density, Phys. Rev. Lett. 98 (2007) 155001. http://dx.doi.org/10.1103/PhysRevLett.98.155001.

[21] P. Amendt, J.D. Colvin, R.E. Tipton, D.E. Hinkel, M.J. Edwards, et al., Indirect-drive noncryogenic double-shell ignition targets for the National Ignition Facility: design and analysis, Phys. Plasmas 9 (2002) 2221. http://dx.doi.org/10.1063/1.1459451.

[22] K. Molvig, M.J. Schmitt, B.J. Albright, E.S. Dodd, N.M. Hoffman, et al., Low fuel convergence path to direct-drive fusion ignition, Phys. Rev. Lett. 116 (2016) 255003. http://link.aps.org/doi/10.1103/PhysRevLett.116.255003.

[23] R.F. Smith, J.H. Eggert, R. Jeanloz, T.S. Duffy, D.G. Braun, et al., Ramp compression of diamond to five terapascals, Nature 511 (2014) 330. http://dx.doi.org/10.1038/nature13526.

[24] V.N. Goncharov, S.P. Regan, E.M. Campbell, T.C. Sangster, P.B. Radha, et al., National direct-drive program on OMEGA and the national ignition facility, Plasma Phys. Control. Fusion 59 (2017) 014008. http://stacks.iop.org/0741-3335/59/i=1/a=014008.

[25] W.L. Kruer, The physics of laser plasma interactions, in: D. Pines (Ed.), Frontiers in Physics, vol. 73, Westview, Boulder, CO, 2003.

[26] C.J. Randall, J.R. Albritton, J.J. Thomson, Theory and simulation of stimulated Brillouin scatter excited by nonabsorbed light in laser fusion systems, Phys. Fluids 24 (1981) 1474. http://dx.doi.org/10.1063/1.863551.

[27] R. Betti, O.A. Hurricane, Inertial-confinement fusion with lasers, Nat. Phys. 12 (2016) 435. http://dx.doi.org/10.1038/nphys3736.

[28] J.F. Myatt, J. Zhang, R.W. Short, A.V. Maximov, W. Seka, et al., Multiple-beam laser−plasma interactions in inertial confinement fusion, Phys. Plasmas 21 (2014) 055501. http://scitation.aip.org/content/aip/journal/pop/21/5/10.1063/1.4878623.

[29] D.T. Michel, A.V. Maximov, R.W. Short, J.A. Delettrez, D. Edgell, et al., Measured hot-electron intensity thresholds quantified by a two-plasmon-decay resonant common-wave gain in various experimental configurations, Phys. Plasmas 20 (2013) 055703. http://dx.doi.org/10.1063/1.4803090.

[30] P. Michel, L. Divol, E.L. Dewald, J.L. Milovich, M. Hohenberger, et al., Phys. Rev. Lett. 115 (2015) 055003. http://link.aps.org/doi/10.1103/PhysRevLett.115.055003.

[31] D.S. Montgomery, Two decades of progress in understanding and control of laser plasma instabilities in indirect drive inertial fusion, Phys. Plasmas 23 (2016) 055601. http://aip.scitation.org/doi/abs/10.1063/1.4946016.

[32] J.D. Lindl, O.L. Landen, J. Edwards, E.I. Moses, J. Adams, et al., Erratum: 'Review of the national ignition campaign 2009−2012' [Phys. Plasmas 21, 020501 (2014)], Phys. Plasmas 21 (2014), 129902(E) http://scitation.aip.org/content/aip/journal/pop/21/12/10.1063/1.4903459.

[33] D.E. Hinkel, L.F. Berzak Hopkins, T. Ma, J.E. Ralph, F. Albert, et al., Development of improved radiation drive environment for high foot implosions at the National Ignition Facility, Phys. Rev. Lett. 117 (2016) 225002. http://link.aps.org/doi/10.1103/PhysRevLett.117.225002.

[34] R.J. Leeper, G.A. Chandler, G.W. Cooper, M.S. Derzon, D.L. Fehl, et al., Target diagnostic system for the national ignition facility, Rev. Sci. Instrum. 68 (1997) 868. http://dx.doi.org/10.1063/1.1147917.

[35] H. Sio, J.A. Frenje, J. Katz, C. Stoeckl, D. Weiner, et al., A particle X-ray temporal diagnostic (PXTD) for studies of kinetic, multi-ion effects, and ion-electron equilibration rates in inertial confinement fusion plasmas at OMEGA (invited), Rev. Sci. Instrum. 87 (2016) 11D701. http://aip.scitation.org/doi/abs/10.1063/1.4961552.

[36] D.T. Michel, V.N. Goncharov, I.V. Igumenshchev, R. Epstein, D.H. Froula, Demonstration of the improved rocket efficiency in direct-drive implosions using different ablator materials, Phys. Rev. Lett. 111 (2013) 245005. http://link.aps.org/doi/10.1103/PhysRevLett.111.245005.

[37] D.S. Clark, M.M. Marinak, C.R. Weber, D.C. Eder, S.W. Haan, et al., Radiation hydrodynamics modeling of the highest compression inertial confinement fusion ignition experiment from the national ignition campaign, Phys. Plasmas 22 (2015) 022703. http://dx.doi.org/10.1063/1.4906897.

[38] W. Seka, D.H. Edgell, J.P. Knauer, J.F. Myatt, A.V. Maximov, et al., Time-resolved absorption in cryogenic and room-temperature direct-drive implosions, Phys. Plasmas 15 (2008) 056312. http://dx.doi.org/10.1063/1.2898405.

[39] J. Zhang, J.F. Myatt, R.W. Short, A.V. Maximov, H.X. Vu, et al., Multiple beam two-plasmon decay: linear threshold to nonlinear saturation in three dimensions, Phys. Rev. Lett. 113 (2014) 105001. http://dx.doi.org/10.1103/PhysRevLett.113.105001.

[40] B. Yaakobi, A.A. Solodov, J.F. Myatt, J.A. Delettrez, C. Stoeckl, et al., Measurements of the divergence of fast electrons in laser-irradiated spherical targets, Phys. Plasmas 20 (2013) 092706. http://aip.scitation.org/doi/full/10.1063/1.4824008.

[41] G. Taylor, The instability of liquid surfaces when accelerated in a direction perpendicular to their planes. I, Proc. R. Soc. Lond. Ser. A 201 (1950) 192. http://rspa.royalsocietypublishing.org/content/201/1065/192.

[42] R. Epstein, S. Skupsky, Anticipated improvement in laser beam uniformity using distributed phase plates with quasirandom patterns, J. Appl. Phys. 68 (1990) 924. http://dx.doi.org/10.1063/1.346655.

[43] R.H. Lehmberg, A.J. Schmitt, S.E. Bodner, Theory of induced spatial incoherence, J. Appl. Phys. 62 (1987) 2680. http://dx.doi.org/10.1063/1.339419.

[44] S. Skupsky, R.W. Short, T. Kessler, R.S. Craxton, S. Letzring, et al., Improved laser-beam uniformity using the angular dispersion of frequency-modulated light, J. Appl. Phys. 66 (1989) 3456. http://dx.doi.org/10.1063/1.344101.

[45] J.E. Rothenberg, Polarization beam smoothing for inertial confinement fusion, J. Appl. Phys. 87 (2000) 3654. http://aip.scitation.org/doi/abs/10.1063/1.372395.

[46] V.N. Goncharov, J.P. Knauer, P.W. McKenty, P.B. Radha, T.C. Sangster, et al., Improved performance of direct-drive inertial confinement fusion target designs with adiabat shaping using an intensity picket, Phys. Plasmas 10 (2003) 1906. http://dx.doi.org/10.1063/1.1562166.

[47] A. Bose, K.M. Woo, R. Betti, E.M. Campbell, D. Mangino, et al., Core conditions for alpha heating attained in direct-drive inertial confinement fusion, Phys. Rev. E 94 (2016), 011201(R). http://journals.aps.org/pre/abstract/10.1103/PhysRevE.94.011201.

[48] R. Nora, R. Betti, K.S. Anderson, A. Shvydky, A. Bose, et al., Theory of hydro-equivalent ignition for inertial fusion and its applications to OMEGA and the National Ignition Facility, Phys. Plasmas 21 (2014) 056316. http://scitation.aip.org/content/aip/journal/pop/21/5/10.1063/1.4875331.

[49] S.P. Regan, V.N. Goncharov, I.V. Igumenshchev, T.C. Sangster, R. Betti, et al., Phys. Rev. Lett. 117 (2016) 025001. http://journals.aps.org/prl/abstract/10.1103/PhysRevLett.117.025001. http://journals.aps.org/prl/abstract/10.1103/PhysRevLett.117.059903. Phys. Rev. Lett. 117 (2016) 059903(E).

[50] I.V. Igumenshchev, V.N. Goncharov, F.J. Marshall, J.P. Knauer, E.M. Campbell, et al., Three-dimensional modeling of direct-drive cryogenic implosions on OMEGA, Phys. Plasmas 23 (2016) 052702. http://scitation.aip.org/content/aip/journal/pop/23/5/10.1063/1.4948418.

[51] P.B. Radha, M. Hohenberger, D.H. Edgell, J.A. Marozas, F.J. Marshall, et al., Direct drive: simulations and results from the national ignition facility, Phys. Plasmas 23 (2016) 056305. http://scitation.aip.org/content/aip/journal/pop/23/5/10.1063/1.4946023.

[52] J.H. Kelly, A. Shvydky, J.A. Marozas, M.J. Guardalben, B.E. Kruschwitz, et al., Simulations of the propagation of multiple-FM smoothing by spectral dispersion on OMEGA EP, in: Proc. SPIE 8602, 2013, p. 86020D. http://proceedings.spiedigitallibrary.org/proceeding.aspx?articleid=1654222.

[53] S.P. Obenschain, D.G. Colombant, M. Karasik, C.J. Pawley, V. Serlin, et al., Effects of thin high-$Z$ layers on the hydrodynamics of laser-accelerated plastic targets, Phys. Plasmas 9 (2002) 2234. http://dx.doi.org/10.1063/1.1464541.

[54] T.J.B. Collins, J.A. Marozas, K.S. Anderson, R. Betti, R.S. Craxton, et al., A polar-drive−ignition design for the National Ignition Facility, Phys. Plasmas 19 (2012) 056308. http://dx.doi.org/10.1063/1.3693969.

[55] F.J. Marshall, P.B. Radha, M.J. Bonino, J.A. Delettrez, R. Epstein, et al., Polar-direct-drive experiments with contoured-shell targets on OMEGA, Phys. Plasmas 23 (2016) 012711. http://scitation.aip.org/content/aip/journal/pop/23/1/10.1063/1.4940939.